Military Technical College
Kobry Elkobbah,
Cairo, Egypt
April 19-21,2016

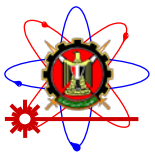

8th International Conference on
Mathematics and Engineering
Physics (ICMEP-8)

PH-1

Investigation of Rainbow like-structure observed in α+^{16}O elastic scattering

Sh. Hamada*
* Faculty of Science, Tanta University, Tanta, Egypt
E-mail: sh.m.hamada@science.tanta.edu.eg

Abstract

the current work aims to study the rainbow like structure observed in the elastic scattering of alpha particles on ^{16}O nuclei. We analyzed the experimental elastic scattering angular distributions data for α+^{16}O nuclear system at energies 49.5, 69.5, 80.7 and 104 MeV. The data were analyzed using both optical potential and double folding potential of different interaction models such as: CDM3Y1, DDM3Y1, CDM3Y6 and BDM3Y1. Potential created by BDM3Y1 interaction model has the shallowest depth which reflects the necessity to use higher renormalization factor. Both optical model and double folding potential of different interaction models reasonably reproduce the experimental data. The obtained renormalization factor is nearly in the range 1.1157 - 1.3312.

Keywords: double folding potential; optical model; density distribution; nuclear rainbow.
PACS number(s): 21.10.Jx, 21.60.Cs, 24.10.Eq, 25.70.Hi

1. Introduction

Study of nuclear interactions is of special interest as it could provide us with useful information about nuclear structure and mechanism of interaction. One of the most interesting features which could be observed in study of nuclear reactions is nuclear rainbow phenomenon. This phenomenon is well observed in elastic scattering of some nuclear system such as ^{16}O+^{12}C [1,2], ^{12}C+^{12}C [3, 4], ^{16}O+^{16}O [5,6] and also in α-nucleus elastic scattering [7,8]. It is well known that nuclear rainbow should be strongest in the elastic scattering channel if a system with small absorption is chosen. Indeed, the elastic scattering angular distributions for these nuclear systems reveal unmistakable refractive features, such as rainbow scattering patterns and broad interference minima ‘‘Airy minima’’ [9]. These refractive features, can be described consistently by using the optical potentials with a deep (several hundreds MeV) real part. The experimental angular distributions for such systems definitely established the fact that: (i) the real part of the light heavy-ion nucleus nucleus optical potential is strongly attractive: the real part of the optical potential is deep. (ii) In some favorable cases (in particular, for the three aforementioned systems), the imaginary part of the potential is weak enough to allow some information to transpire from the nuclear interior in the elastic scattering differential cross section. The combination of these

two features makes possible the observation in the elastic scattering data of distinctive refractive effects like strong Airy minima.

In the present, we analyzed the $\alpha+^{16}O$ angular distributions at energies 49.5, 69.5, 80.7 and 104 MeV using both optical model (OM) and double folding (DF) potential of different interaction models such as: CDM3Y1, CDM3Y6, DDM3Y1 and BDM3Y1. We have extracted the renormalization factor N_r for $\alpha+^{16}O$ nuclear system at the different concerned energies within the framework of the different concerned interaction models.

The paper is organized as follows. In Sec. 2 the theoretical analysis of the experimental data is presented and Sec. 3 devoted to the results and discussion. The summary is given in Sec. 4.

2. Theoretical Analysis

A. Optical model calculations

The data on elastic scattering were firstly analyzed within the framework of the standard optical model of the nucleus. In this model the elastic scattering is often described by a complex interaction potential with a radial dependence in the form of Woods-Saxon. Parameters of optical potential (OP) were selected to achieve the best agreement between theoretical and experimental angular distributions. In optical model calculations, the differential cross section could be easily calculated as the square of scattering amplitude $\frac{d\sigma}{d\Omega} = |f(\theta,\varphi)|^2$.

Woods-Saxon form factor was taken for both the real and imaginary parts of the potential, and Coulomb potential of a uniform charged sphere.

$$U(r) = V_C - V_0\left[1+\exp\left(\frac{r-R_V}{a_V}\right)\right]^{-1} - iW\left[1+\exp\left(\frac{r-R_W}{a_W}\right)\right]^{-1} \quad (1)$$

with radius

$$R_i = r_i(A_T^{1/3}), \qquad i = V, W, C$$

Elastic nucleus-nucleus scattering amplitude can be expressed in the following form

$$f(\theta) = f_c(\theta) + \frac{i}{2k}\sum_l (2l+1)\exp(2i\sigma_l)(1-S_l)P_l(\cos\theta), \quad (2)$$

where $f_c(\theta)$ is the amplitude of the Coulomb scattering, σ_l - the Coulomb phase shift, k - the wave number, S_l - the scattering matrix element for the l-th partial wave, and $P_l(\cos\theta)$ - the Legendre polynomial.

It is frequently found that many sets of parameters give equally good fits to the data, and the question then arises whether any one of these is more physical than the others and if so which is to be preferred. These parameter ambiguities, as they are called, are of two main types, discrete and continuous. Discrete ambiguities refer to regions of parameter space that give acceptable fits separated by unacceptable regions. Continuous ambiguities refer to combinations of parameters that may be simultaneously varied being subjected to some constraint without significantly affecting the fit. The existence of these and other more complicated parameter ambiguities means that it is not possible to establish the optical potential by phenomenological analyses alone. It is necessary to start by constraining the potential

as closely as possible by physical requirements before parameter optimization. So, it is preferable to use more microscopic models such as double folding.

B. Elastic scattering in the framework of double folding

The double folding potential of different interaction models such as: (CDM3Y1, DDM3Y1, CDM3Y6 and BDM3Y1) for $\alpha+^{16}O$ nuclear system at energies (49.5, 69.5, 80.7 and 104 MeV) was prepared using code DFMSPH [10]. All these different interaction models are essentially based on the basic form of M3Y Reid or M3Y Paris, but the main difference between them lies in the values of the parameters used in calculating density-dependent function *F(ρ)*. Figure 1 shows co-ordinate system for the double folding model.

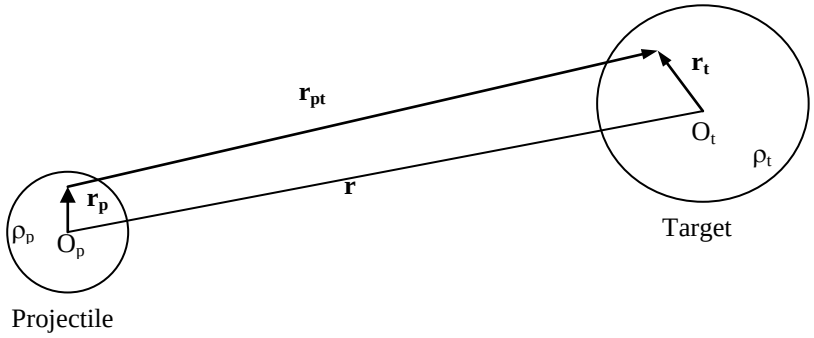

Fig. 1: shows co-ordinate system for the double folding model

In the double folding calculations, the real part of the potential is calculated using the double folding method in which the nucleon-nucleon (*NN*) interaction potential $v_{NN}(s)$ is folded into the densities of the projectile $\rho_p(r_p)$ and target nuclei $\rho_t(r_t)$. The effective *NN* interaction potential was taken to be of the CDM3Y1 and CDM3Y6 forms based on the M3Y-Paris potential:

$$v_{\mathrm{D}}(s) = 11061.625\frac{\exp(-4s)}{4s} - 2537.5\frac{\exp(-2.5s)}{2.5s},$$
$$v_{\mathrm{EX}}(s) = -1524.25\frac{\exp(-4s)}{4s} - 518.75\frac{\exp(-2.5s)}{2.5s} - 7.8474\frac{\exp(-0.7072s)}{0.7072s}, \quad (3)$$

and also was taken to be of the BDM3Y1 and DDM3Y1 forms based on the M3Y-Reid potential:

$$v_{\mathrm{D}}(s) = 7999.0\frac{\exp(-4s)}{4s} - 2134.25\frac{\exp(-2.5s)}{2.5s}, \quad (4)$$

$$v_{\mathrm{EX}}(s) = -4631.38\frac{\exp(-4s)}{4s} - 1787.13\frac{\exp(-2.5s)}{2.5s} - 7.8474\frac{\exp(-0.7072s)}{0.7072s},$$

The M3Y-Paris and M3Y- Reid interactions are scaled by an explicit density-dependent function *F(ρ)*:

$$v_{\mathrm{D(EX)}}(\rho, s) = F(\rho)v_{\mathrm{D(EX)}}(s), \quad (5)$$

where $v_{D(EX)}$ are the direct and exchange components of the M3Y-Paris and M3Y-Reid, ρ is the nuclear matter (*NM*) density. Density-dependent function *F(ρ)*, was taken to be exponential dependence, and the parameters were adjusted to reproduce the *NM* saturation properties in the HF calculation. The density-dependent function can be written as:

$$F(\rho) = C[1 + \alpha \exp(-\beta\rho) - \gamma\rho^n], \quad (6)$$

the parameters *C, α, β, γ* for the different concerned interaction models listed in table 1 were taken from [11].

Table 1 – Parameters of density-dependence function *F(ρ)*

Interaction Model	c	α	β (fm^3)	γ (fm^{3n})	n	*K* (MeV)
CDM3Y6	0.2658	3.8033	1.4099	4.0	1	252
CDM3Y1	0.3429	3.0232	3.5512	0.5	1	188
BDM3Y1	1.2253	0.0	0.0	1.5124	1	232
DDM3Y1	0.2845	3.6391	2.9605	0.0	0	171

The density distribution of α and ^{16}O is expressed in a modified form of the Gaussian shape as $\rho(r) = \rho_0(1 + wr^2)\exp(-\beta r^2)$, where ($\rho_0$=0.4229, w=0.0, β=0.7024) for α particles [12] and (ρ_0=0.1317, w=0.6457, β=0.3228) for ^{16}O [13].

3. Results and discussion

The comparisons between the experimental data for α+^{16}O nuclear system at energies (49.5, 69.5, 80.7 and 104 MeV) **[**14-16**]** and the theoretical calculations within the framework of optical model is shown in figure 2. Both the phenomenological (Optical Model) and semi microscopic (Double Folding) calculations were performed using code FRESCO and code SFRESCO [17]. The radius parameter for real volume part of potential (r_V) was fixed at 1.36 fm, radius parameter for imaginary volume part of potential (r_W) was fixed at 1.73 fm and radius parameter for the Coulomb part of potential (r_C) was fixed at 1.25 fm. The optimal optical potential parameters are listed in table 2.

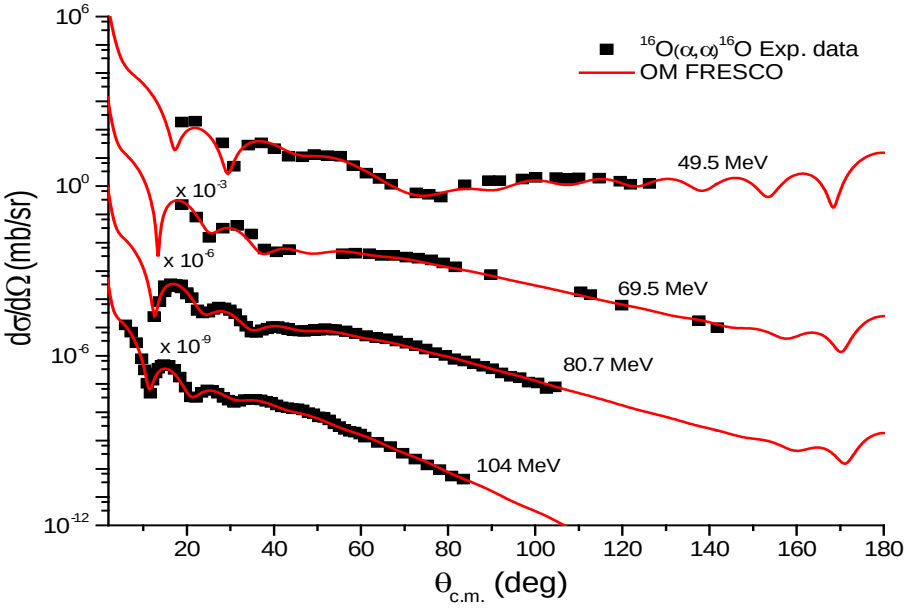

Fig. 2: The comparison between the experimental data for α +^{16}O at energies (49.5, 69.5, 80.7 and 104 MeV) and the theoretical calculations within the framework of optical model

The comparison between the experimental data for α+^{16}O at energies (49.5, 69.5, 80.7 and 104 MeV) and the double folding calculations of different interaction models: CDM3Y1, DDM3Y1, CDM3Y6 and BDM3Y1 are shown in figures 3, 4, 5 and 6 respectively. Optimal potential parameters for α+^{16}O nuclear system, also those from double folding of different interaction models are listed in table 2. The obtained renormalization factor (N_r) for α+^{16}O nuclear system is in the range 1.1157 - 1.3312. The imaginary part of the potential was taken in the form of standard Woods-Saxon form factor, the same parameter of the imaginary part of potential were kept constant during the double folding calculations. So, the nuclear potential in this case has the following shape:

$$U(R) = V_C + Nr\,V^{DF}(R) + iW(R) \qquad (7)$$

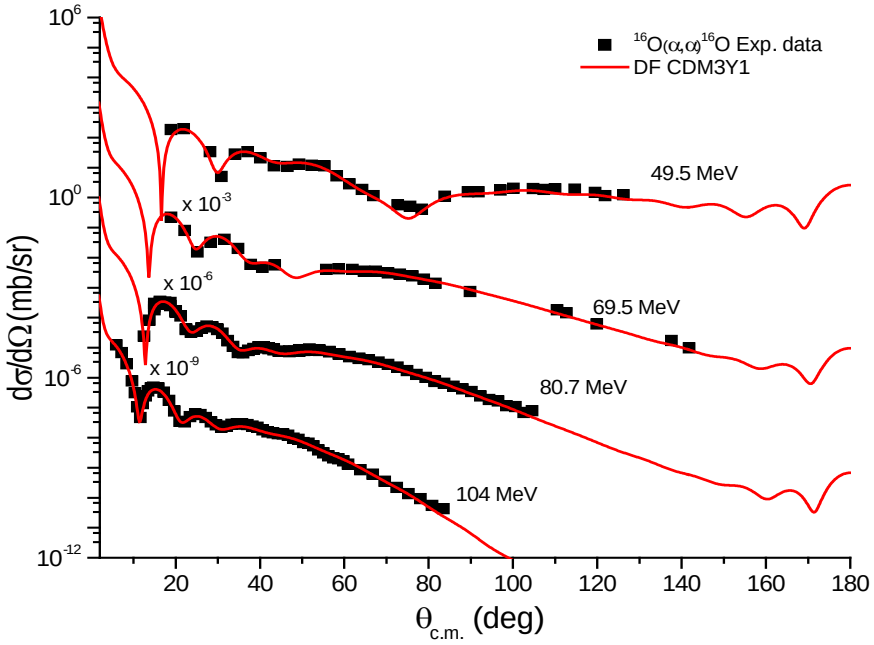

Fig. 3: The comparison between the experimental data for $\alpha + {}^{16}O$ at energies (49.5, 69.5, 80.7 and 104 MeV) and the theoretical calculations using double folding potential of interaction model CDM3Y1.

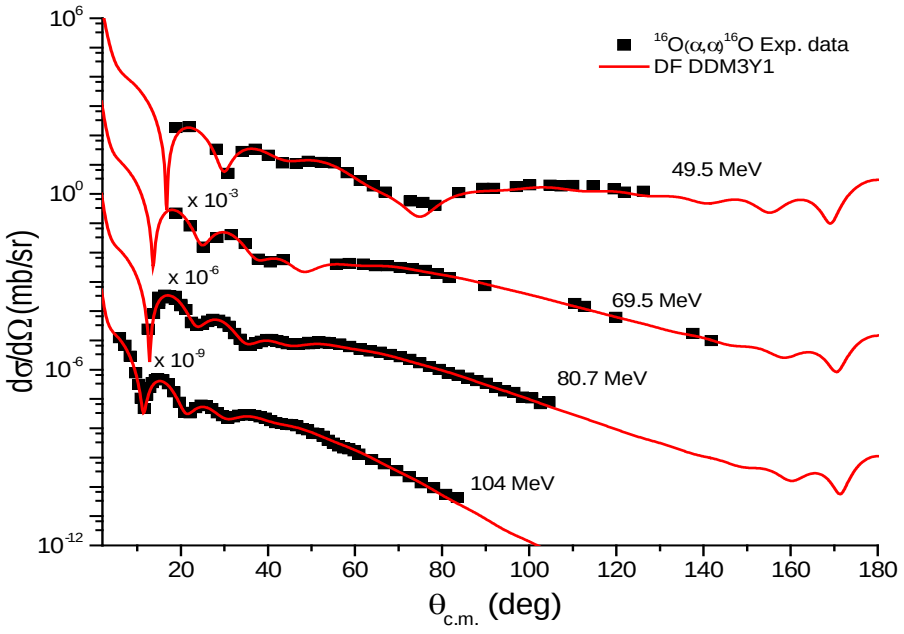

Fig. 4: the same as figure 3 but for interaction model DDM3Y1

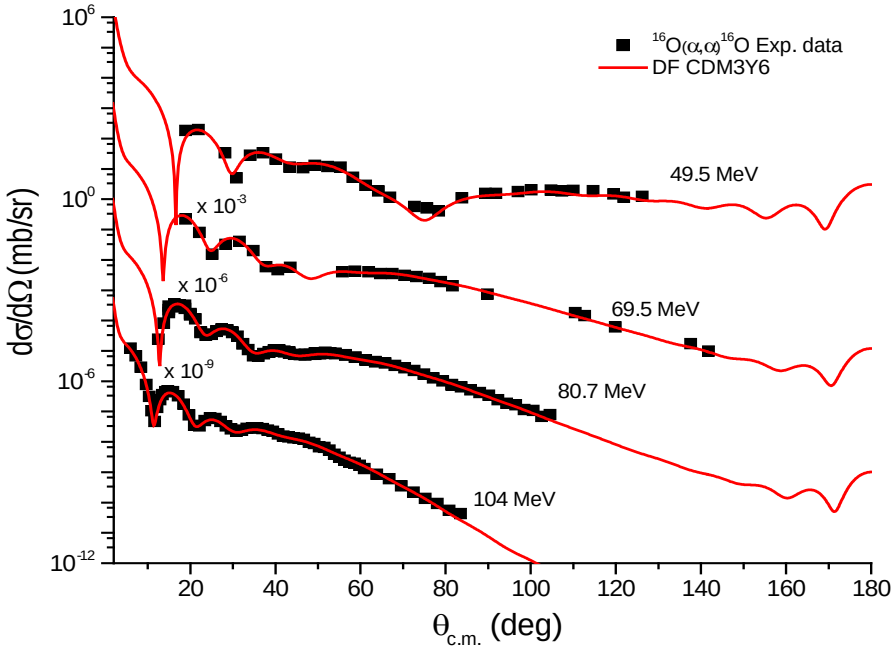

Fig. 5: the same as figure 3 but for interaction model CDM3Y6

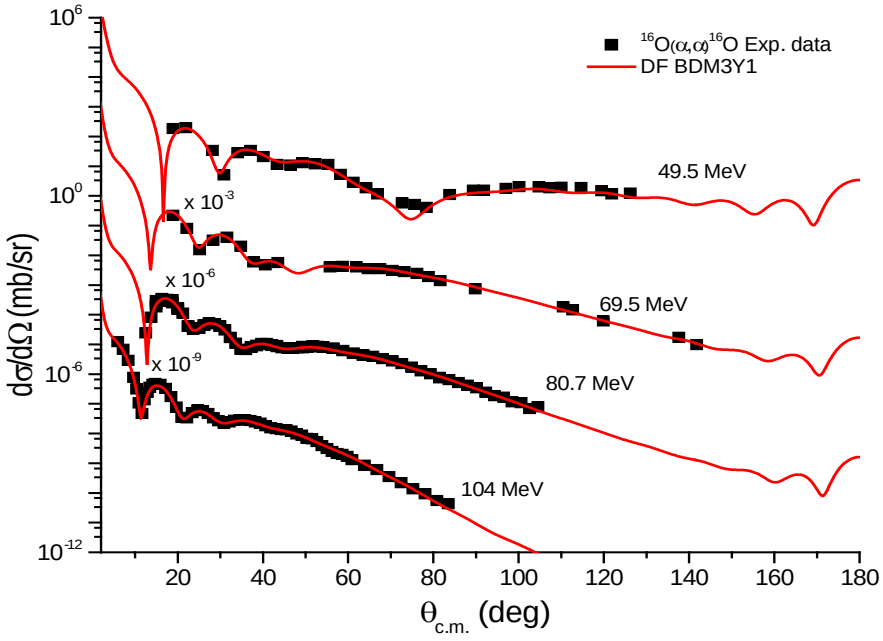

Fig. 6: the same as figure 3 but for interaction model BDM3Y1

Table 2 – Optical potential and double folding parameters for α-particles elastically scattered on ^{16}O at different energies

E (MeV)	Model	V_o (MeV)	a_v (fm)	W_o (MeV)	a_w (fm)	N_r
49.5	OM	109.63	0.6	8.94	0.739	
	DF- CDM3Y1			8.94	0.739	1.1228
	DF- DDM3Y1			8.94	0.739	1.1474
	DF- CDM3Y6			8.94	0.739	1.1931
	DF- BDM3Y1			8.94	0.739	1.2143
69.5	OM	99.99	0.715	15.58	0.648	
	DF- CDM3Y1			15.58	0.648	1.1209
	DF- CDM3Y6			15.58	0.648	1.1782
	DF- DDM3Y1			15.58	0.648	1.1458
	DF- BDM3Y1			15.58	0.648	1.2002
80.7	OM	101.26	0.714	16.7	0.556	
	DF- CDM3Y1			16.7	0.556	1.1307
	DF- DDM3Y1			16.7	0.556	1.1637
	DF- CDM3Y6			16.7	0.556	1.191
	DF- BDM3Y1			16.7	0.556	1.2225
104	OM	93.25	0.731	17.25	0.541	
	DF- CDM3Y1			17.25	0.541	1.1157
	DF- DDM3Y1			17.25	0.541	1.2687
	DF- CDM3Y6			17.25	0.541	1.1717
	DF- BDM3Y1			17.25	0.541	1.3312

As we discussed before, the calculations has performed in this work using different four models of interaction: CDM3Y1, CDM3Y6, BDM3Y1 and DDM3Y1, and the used double folding potential consists of two parts direct part and exchange part. Figure 7 shows the variation of the potential depth with radius for the direct and exchange parts of the potential and also their sum (direct+exchange). Figure 8, shows how is the potential created by BDM3Y1 model of interaction is shallower in comparison with the rest which reflect the necessity to use higher normalization factor.

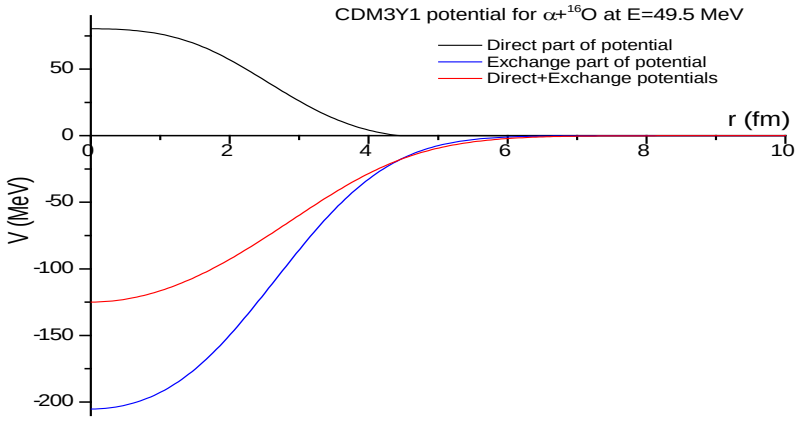

Fig. 7: Shows the variation of the potential depth with radius for both direct and exchange parts of the potential and also their sum (direct+exchange) at E=49.5 MeV.

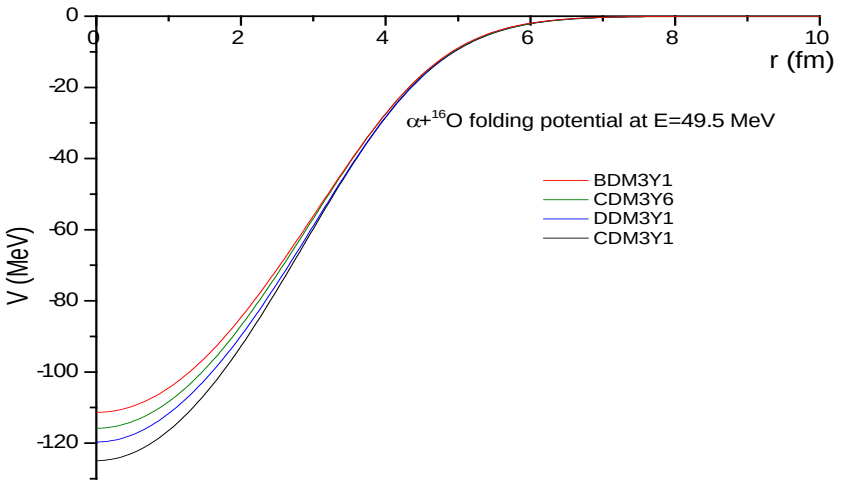

Fig. 8: Shows the variation of the potential depth with radius for $\alpha+^{16}O$ folding potential at E=49.5 MeV using different models of interaction CDM3Y1, DDM3Y1, CDM3Y6 and BDM3Y1.

The nuclear rainbow phenomenon could be clearly observed in $^{16}O(\alpha,\alpha)^{16}O$ elastic scattering at the aforementioned energies. The characteristic features of the falloff of the cross section beyond the rainbow angle in the experimental angular distributions are well reproduced. Both optical model and double folding of different interaction models (CDM3Y1, DDM3Y1, CDM3Y6 and BDM3Y1) could reasonably reproduce the experimental data. Double folding calculations expected that the Airy minimum is$\approx 48^{o}$ at E=69.5 MeV as shown in figures 3-6, while from the optical model calculations it is around 40^{o} as shown in figure 2, the minimum$\approx$at 48^{o} couldn't be observed from experimental data. The angular distribution data at energy 49.5 MeV showed that the Airy minimum is$\approx 78^{o}$, but the DF calculations expected the minimum to be$\approx 75^{o}$ and this may be due to the existence of a valley of two minima: the first minimum at 78^{o} as shown in Fig. 2 and the second probably at 70^{o} (not shown in the experimental data). At energies 80.7 and 104 MeV, both OM and DF calculations expected the same position for Airy minimum (35^{o} at E=80.7 MeV and 31^{o} at E=104 MeV). As shown in figures 2-6, with increasing the energy of the incident projectile, the position of rainbow angle is shifted toward small angles. The angular position of rainbow angle at the different concerned energies is shown in figure 9.

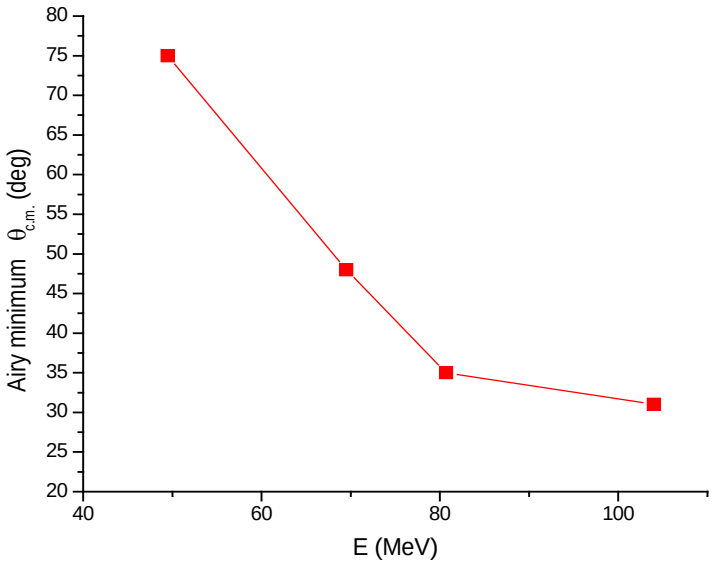

Fig. 9: Angular position of the Airy minimum for $\alpha+^{16}O$ elastic scattering at energies 49.5, 69.5, 80.7 and 104 MeV. The lines are only to guide the eye.

4. Summary

We analyzed the experimental angular distributions for $\alpha+^{16}O$ nuclear system at energies 49.5, 69.5, 80.7 and 104 MeV using both optical potential: where the real and imaginary parts of the potential have Woods-Saxon shape and double folding potential of different interaction models. Refractive features and nuclear rainbow phenomenon is well presented in the experimental data and will reproduced using both OP and DFP. Analysis of experimental data using double folding potential of different interaction models CDM3Y1, DDM3Y1, CDM3Y6 and BDM3Y1 showed that, the potential created by BDM3Y1 interaction model has the shallowest depth which reflects the necessity to use higher renormalization factor, and the potential created by CDM3Y1 model of interaction is the deepest which reflects the necessity to use smaller renormalization factor. The obtained renormalization factor using all the aforementioned interaction models is in the range 1.1157 - 1.3312.

References

1 M.P.Nicoli, F.Haas, R.M.Freeman, S.Szilner, Z.Basrak, A.Morsad, G.R.Satchler and M. E. Brandan, Phys. Rev. C 61(2000) 034609.
2 A. A. Ogloblin, D. T. Khoa, Y. Kondo, Yu. A. Glukhov, A. S. Dem'yanova, M. V. Rozhkov, G. R. Satchler and S. A. Goncharov, Phys. Rev. C 57 (1998) 1797.
3 M. P. Nicoli, F. Haas, R. M. Freeman, N. Aissaoui, C. Beck, A. Elanique, R. Nouicer, A. Morsad, S. Szilner, Z. Basrak, M. E. Brandan, G. R. Satchler, Phys. Rev. C 60 (1999) 064608.
4 D. T. Khoa, von Oertzen W., H. G. Bohlen and F. Nuoffer, Nucl. Phys. A 672 (2000) 387.
5 C.-C. Sahm, T. Murakami, J. G. Cramer, A. J. Lazzarini, D. D. Leach, D. R. Tieger , R. A. Loveman, W. G. Lynch, M. B. Tsang and J. Van der Plicht, Phys. Rev. C 34 (1986) 2165.
6 M. E. Brandan, Phys. Rev. Lett.60.784.
7 M. El-Azab Farid, Z. M. M. Mahmoud, and G. S. Hassan, Phys. Rev. C 64 (2001) 014310
8 Dao T. Khoa, Phys. Rev. C 63 (2001) 034007
9 D. A. Goldberg and S. M. Smith, Phys. Rev. Lett. 33 (1974) 715.

10 I. I. Gontchar, M. V. Chushnyakova Computer Physics Communications 181 (2010) 168–182.
11 D. T. Khoa et al., Phys. Rev. C56(1997) 954.
12 G.R. Satchler, W.G. Love, Phys. Rep. 55 (1979) 183.
13 S. Qing-biao, F. Da-chun and Z. Yi-Zhong, Phys. Rev. C 43(1991) 2773.
14 F. Michel, J. Albinski, P. Belery, Th. Delbar, Gh. Gregoire, B. Tasiaux, G. Reidemeister, ., Phys. Rev. C 28(1983) 1904
15 T,REED,69-14,1968) Technical report
16 G. Hauser, R. Lohken, H. Rebel, G. Schatz, G. W. Schweimer, J. Specht, Nucl. Phys. A 128 (1969) 81.
17 I. J. Thompson, Comput. Phys. Rep. 7 (1988) 167.